

# Mutants, Overexpressors, and Interactors of Arabidopsis Plastocyanin Isoforms: Revised Roles of Plastocyanin in Photosynthetic Electron Flow and Thylakoid Redox State

Paolo Pesaresi<sup>a</sup>, Michael Scharfenberg<sup>b</sup>, Martin Weigel<sup>c</sup>, Irene Granlund<sup>d</sup>, Wolfgang P. Schröder<sup>d</sup>, Giovanni Finazzi<sup>e</sup>, Fabrice Rappaport<sup>e</sup>, Simona Masiero<sup>f</sup>, Antonella Furini<sup>g</sup>, Peter Jahns<sup>h</sup> and Dario Leister<sup>b,1</sup>

<sup>a</sup> Dipartimento di Produzione Vegetale, Università degli studi di Milano c/o Parco Tecnologico Padano Via Einstein, Loc. Cascina Codazza, I-26900 Lodi, Italy

<sup>b</sup> Lehrstuhl für Botanik, Department Biologie I, Ludwig-Maximilians-Universität München, Großhaderner Str. 2, D-82152 Planegg-Martinsried, Germany

<sup>c</sup> Abteilung für Pflanzenzüchtung und Genetik, Max-Planck-Institut für Züchtungsforschung, Carl-von-Linné-Weg 10, D-50829 Köln, Germany

<sup>d</sup> Institute of Chemistry and Umeå Plant Science Centre (UPSC), Umeå University, SE-901 87 Umeå, Sweden

<sup>e</sup> Institut de Biologie Physico-Chimique, UMR 7141 CNRS-Université P. et M. Curie, 13, rue Pierre et Marie Curie, F-75005 Paris, France

<sup>f</sup> Dipartimento di Biologia, Università degli studi di Milano, Via Celoria 26, I-20133 Milano, Italy

<sup>g</sup> Dipartimento Scientifico e Tecnologico, Università degli studi di Verona, Strade le Grazie 15, I-37134 Verona, Italy

<sup>h</sup> Institut für Biochemie der Pflanzen, Heinrich-Heine-Universität Düsseldorf, Universitätsstr. 1, D-40225 Düsseldorf, Germany

**ABSTRACT** Two homologous plastocyanin isoforms are encoded by the genes PETE1 and PETE2 in the nuclear genome of *Arabidopsis thaliana*. The PETE2 transcript is expressed at considerably higher levels and the PETE2 protein is the more abundant isoform. Null mutations in the PETE genes resulted in plants, designated pete1 and pete2, with decreased plastocyanin contents. However, despite reducing plastocyanin levels by over 90%, a pete2 null mutation on its own affects rates of photosynthesis and growth only slightly, whereas pete1 knockout plants, with about 60–80% of the wild-type plastocyanin level, did not show any alteration. Hence, plastocyanin concentration is not limiting for photosynthetic electron flow under optimal growth conditions, perhaps implying other possible physiological roles for the protein. Indeed, plastocyanin has been proposed previously to cooperate with cytochrome  $c_{6A}$  (Cyt  $c_{6A}$ ) in thylakoid redox reactions, but we find no evidence for a physical interaction between the two proteins, using interaction assays in yeast. We observed homodimerization of Cyt  $c_{6A}$  in yeast interaction assays, but also Cyt  $c_{6A}$  homodimers failed to interact with plastocyanin. Moreover, phenotypic analysis of atc6-1 pete1 and atc6-1 pete2 double mutants, each lacking Cyt  $c_{6A}$  and one of the two plastocyanin-encoding genes, failed to reveal any genetic interaction. Overexpression of either PETE1 or PETE2 in the pete1 pete2 double knockout mutant background results in essentially wild-type photosynthetic performance, excluding the possibility that the two plastocyanin isoforms could have distinct functions in thylakoid electron flow.

## INTRODUCTION

Plastocyanin is a soluble copper-binding protein located in the thylakoid lumen and serves as an electron carrier from cytochrome  $f$  (Cyt  $f$ ) in the cytochrome  $b_{6/f}$  complex (Cyt  $b_{6/f}$ ) to  $P_{700}^+$  in photosystem I (PSI) (Katoh, 1960; Gorman and Levine, 1965; for a review, see Redinbo et al., 1994). Plastocyanin levels depend on various conditions, and a close correlation between plastocyanin contents and photosynthetic electron transport activity has been reported. For instance, in barley, the size of the plastocyanin pool correlates with photosynthetic electron transport activity (Burkey, 1993), and, in tobacco, the photosynthetic electron flux is sensitive to variations in the amount of plastocyanin relative to PSI and Cyt  $b_{6/f}$  (Schöttler

et al., 2004). Moreover, intra-specific variation in photosynthetic electron transport is linked to differences in plastocyanin content in tall fescue (Krueger et al., 1984), barley (Burkey, 1994), and soybean (Burkey et al., 1996).

Recently, the strict association of photosynthetic performance and plastocyanin content has been challenged by

mutant analyses in *Arabidopsis thaliana*. In the paa1 and paa2 mutants, affected in Cu transport over plastid envelope and thylakoid membranes, respectively (Shikanai et al., 2003; Abdel-Ghany et al., 2005), even drastic reductions in plastocyanin contents resulted in only mild alterations in thylakoid electron flow. Moreover, *A. thaliana* RNA interference (RNAi) lines without detectable plastocyanin levels still reached a plant height of 50% with respect to wild-type (WT) plants (Gupta et al., 2002). This implies that even relatively low amounts of plastocyanin are capable of supporting efficient electron transport rates under optimal growth conditions.

Besides its role as an inter-systemic electron carrier, additional functions for plastocyanin have been proposed recently. Thus, plastocyanin and Cyt c<sub>6A</sub>, a Cyt c<sub>6</sub>-like protein (Gupta et al., 2002; Wastl et al., 2002), might cooperate within the thylakoid lumen in the redox-dependent modulation of luminal protein activities (Schlarb-Ridley et al., 2006). In detail, Cyt c<sub>6A</sub> could donate electrons derived from the formation of disulphide bridges in thylakoid lumen proteins to plastocyanin, whereas in the absence of Cyt c<sub>6A</sub>, the target protein(s) might be oxidized directly by plastocyanin. In contrast to the stromal ferredoxin–thioredoxin system, this hypothetical mechanism would activate thylakoid proteins upon illumination by oxidation rather than by reduction (Buchanan and Luan, 2005). Consistent with this model, rapid electron transfer between Cyt c<sub>6A</sub> and plastocyanin has been observed in vitro (Marcaida et al., 2006). A major role in copper (Cu) homeostasis has also been proposed for plastocyanin (Märschner, 2002; Puig et al., 2007).

Several angiosperms, including *A. thaliana* (Kieselbach et al., 2000), poplar (Shosheva et al., 2005), parsley (Dimitrov et al., 1990), tobacco (Dimitrov et al., 1993), rice (Yu et al., 2005), and the moss *Physcomitrella patens* (Rensing et al., 2008), express two plastocyanin isoforms. This feature seems to be the result of a relatively recent evolutionary event, characteristic of land plants, because only one plastocyanin isoform has been detected in cyanobacteria and algae, such as *Synechocystis* and *Chlamydomonas* (Merchant and Bogorad, 1987; Briggs et al., 1990). In vitro, the two poplar plastocyanin isoforms have different electrostatic properties, melting temperatures, and unfolding enthalpies (Shosheva et al., 2004, 2005), but it is not clear whether these differences are functionally relevant in planta.

In this work, we have investigated to which degree plastocyanin amounts can limit the photosynthetic electron flow in *A. thaliana* and whether the two plastocyanin isoforms exhibit functional differences by employing knockout and overexpressing lines for each isoform. The data clearly indicate that the two *Arabidopsis* plastocyanins have redundant functions in photosynthetic electron transport, and accumulate in thylakoids to levels higher than those necessary to support efficient photosynthetic electron flow. Additional experiments imply that plastocyanin does not interact with Cyt c<sub>6A</sub>, either functionally or physically. However, reduced plastocyanin levels drastically increase the susceptibility of plants to Cu stress, implying that the protein does play a major role as a Cu sink.

## RESULTS

### Sequence Analysis of PETE1 and PETE2

In *A. thaliana*, plastocyanin is encoded by two genes—PETE1 (At1g76100) and PETE2 (At1g20340)—which show 73% identity at the DNA level (Weigel et al., 2003). Both genes are located on chromosome 1, and inspection of the level of synteny between the chromosomal regions surrounding the two genes indicated that PETE1 and PETE2 result from a relatively recent segmental duplication in the *Arabidopsis* lineage (Blanc et al., 2003; <http://wolfe.gen.tcd.ie/athal/dup>).

PETE1 and PETE2 code for homologous proteins, which share 82/92% identity/similarity. After cleavage of the bipartite transit peptides, the mature proteins differ in 18 of 99 amino acid residues, with more than half of the substitutions being conservative replacements (Figure 1). They also show high degrees of identity/similarity with plastocyanins from other flowering plants, moss, algae, and cyanobacteria. In particular, the hydrophobic surface formed by residues G10, L12, G34, F35, and A90, which is important for interactions with redox partners (Haehnel et al., 1994; Olesen et al., 1999), is highly conserved in plant and algal plastocyanins and partially also in cyanobacteria (see circles in Figure 1). Residues Y83 and H87 are involved in the two possible routes for electron transfer (Taneva et al., 2000), and are also strictly conserved in all plastocyanin protein sequences displayed in Figure 1 (see + symbols). Moreover, the acidic patch formed by residues 42–44 (see asterisks in Figure 1), thought to be involved in the reaction with PSI (Haehnel et al., 1994; Olesen et al., 1999), is almost totally maintained in flowering plants, moss, algae, and bacteria. Clearly, their high degree of homology, especially in the domains involved in interactions and electron transfer between Cyt b<sub>6</sub>/f and PSI, points to conserved functions for both plastocyanin isoforms in *A. thaliana*.

### A Large Excess of Plastocyanin is Present in the Thylakoid Lumen of *Arabidopsis* Plants

To investigate whether the plastocyanin pool size plays a critical role in regulating thylakoid electron flow, En-transposon insertion mutants were isolated for both plastocyanin-encoding genes (Weigel et al., 2003). Quantitative reverse-transcription PCR (QRT-PCR), designed to discriminate between PETE1 and PETE2 transcripts, indicated that PETE2 mRNA was 10 times more abundant than PETE1 transcripts in WT leaves (Figure 2). In the pete1-1 (pete1::En1) mutant, PETE1 transcript accumulation was completely suppressed, while in pete2-1 (pete2::En1), residual amounts of PETE2 transcript were present, most probably due to somatic En-transposon excision events. However, no change in the expression of the remaining functional plastocyanin-encoding gene was detected in either of the single mutants.

Stable pete1-1.1 (abbreviated in the following as pete1) and pete2-1.1 (abbreviated as pete2) null alleles, bearing frame-shift mutations, were obtained after germline transposon excision (Weigel et al., 2003), and analyzed for their growth rate,

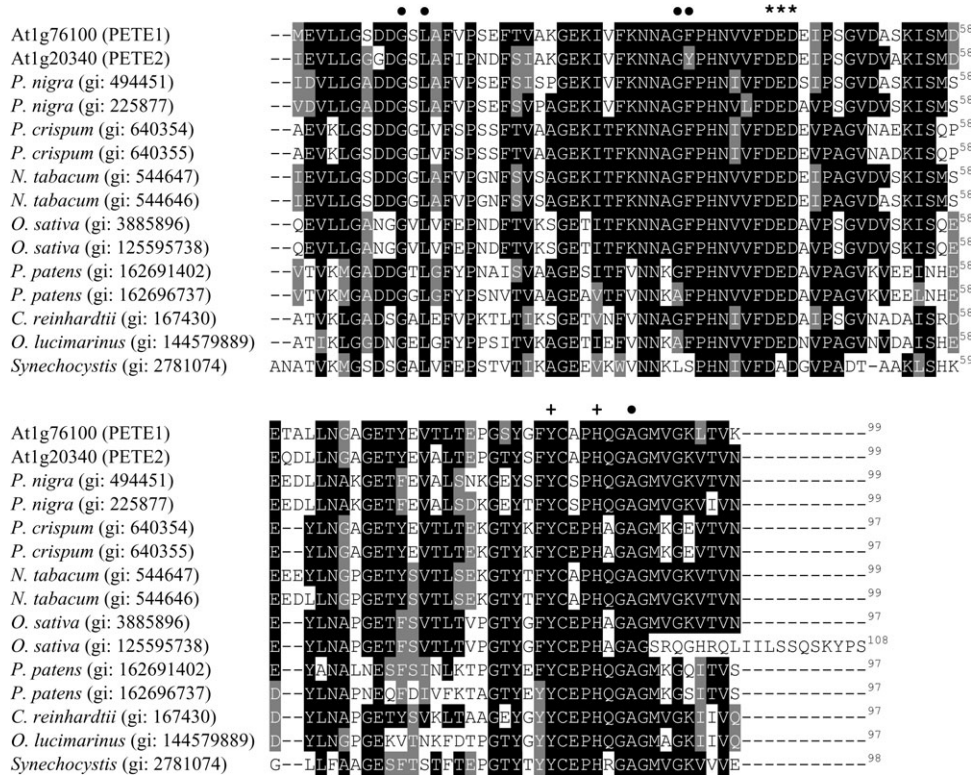


Figure 1. Comparison of Mature Plastocyanin Sequences from Flowering Plants, Moss, Algae, and Cyanobacteria.

The amino acid sequence of the *Arabidopsis* PETE1 protein (At1g76100) was compared with the PETE2 sequence (At1g20340) and with other plastocyanin sequences from *Populus nigra* (gi:494451; gi:225877), *Petroselinum crispum* (gi:640354; gi:640355), *Nicotiana tabacum* (gi:544647; gi:544646), *Oryza sativa* (gi:3885896; gi:125595738), *Physcomitrella patens* (gi:162691402; gi:162696737), *Chlamydomonas reinhardtii* (gi:167430), *Ostreococcus lucimarinus* (gi:144579889), and *Synechocystis* sp. PCC 6803 (gi:2781074). Black boxes indicate strictly conserved amino acids, and grey boxes closely related ones. The characteristic hydrophobic patch, essential for the interactions with redox partners (see circles), is indicated according to Olesen et al. (1999). The tyrosine and histidine residues (see '+' symbol), involved in electron transfer are indicated according to Taneva et al. (2000). The asterisks refer to the acidic patch (Olesen et al., 1999).

photosynthetic performances, and plastocyanin content. Whereas *pete1* mutants developed similarly to WT, *pete2* lines exhibited a decrease in growth by about 30% (Figure 3). The effective quantum yield of PSII ( $U_{II}$ ), measured under an actinic light intensity of  $80 \text{ } \mu\text{mol m}^{-2} \text{ s}^{-1}$ , was altered slightly in the *pete2* mutant, while no impairment could be observed in *pete1* leaves (WT:  $0.76 \pm 0.01$ ; *pete1*:  $0.75 \pm 0.01$ ; *pete2*:  $0.67 \pm 0.01$ ). A similar behavior could be observed for the rate of electron transport (ETR) measured under different actinic light intensities (Table 1). Western analyses showed minor reductions (10–30%) in the abundance of the major thylakoid multiprotein complexes only in *pete2* (Figure 4 and Table 2), implying no major alterations in photosynthetic electron flow.

Because the abundance of the thylakoid multiprotein complexes is only weakly affected in *pete2* (see Figure 4 and Table 2), the impairment in linear electron transport might result from an alteration in the rate of plastocyanin-mediated electron transport between Cyt b<sub>6</sub>/f and PSII. To investigate this aspect further, the absorption changes associated with P<sub>700</sub><sup>+</sup> reduction and Cyt f oxidation following a single turnover flash were analyzed in dark-adapted leaves from the two single

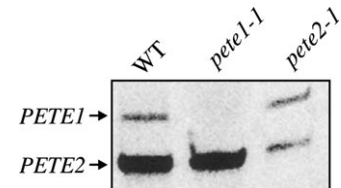


Figure 2. Plastocyanin Expression Analyses.

Detection of PETE transcripts in light-adapted transposon insertion mutants (*pete1-1* and *pete2-1*) and WT plants. The analysis on 4.5% PA gels was performed with <sup>33</sup>P-labeled products of quantitative reverse transcriptase–PCR (QRT-PCR) obtained from leaves after PCR for 25 cycles with PETE-specific primers. Primers specific for the ACTIN1 gene were used in the same PCR reaction to check for equal loading (data not shown). The assay was confirmed to be quantitative by testing dilution series for each sample (data not shown).

mutants (Figure 5). Under these conditions, the rate of Cyt f oxidation and P<sub>700</sub><sup>+</sup> reduction is strictly proportional to the efficiency of plastocyanin-mediated electron transfer between the two complexes and independent of the relative absorption

cross-section of PSI and of the redox state of the intersystem electron flow (Finazzi et al., 2005). The pete1 and WT plants were characterized by a fast unresolved phase accounting for about 60% of the absorption decay, followed by a slow phase developing over hundreds of 1s, but the pete2 mutant displayed a distinct delay in  $P_{700}^+$  reduction ( $t_{1/2}$ :  $\approx 1$  ms) (Figure 5A). The picture observed for Cyt f oxidation (Figure 5B) was consistent with the kinetic data for  $P_{700}^+$  reduction: in WT, the kinetic profile of Cyt f oxidation consists of a fast phase ( $t_{1/2}$ :  $\approx 100$  1s) with an amplitude that accounts for 75% of the absorption decay, and a slow phase with a half-time decay of about 1 ms and an amplitude of 25%, as previously described (Joliot and Joliot, 2002). However, the amplitude of the slow phase was slightly increased (be-

tween 25 and 45%) in pete1, and became dominant (between 85 and 95%) in pete2. Since the fast ( $\approx 100$  1s) reduction of  $P_{700}^+$  is commonly interpreted as reflecting rapid electron transfer between pre-bound plastocyanin and  $P_{700}^+$  (Farah et al., 1995), the marked slowdown in  $P_{700}^+$  reduction observed in the pete2 mutant may simply result from the absence of pre-bound plastocyanin in this genotype, rather than from significant differences between the intrinsic rate constants of electron transfer from PETE2 or PETE1 to  $P_{700}^+$ . In agreement with this, oxidation of Cyt f was also slowed significantly, as in *C. reinhardtii* mutants lacking the F subunit of PSI, which is involved in the docking of plastocyanin to its oxidation site (Farah et al., 1995). In addition, as will be discussed below, these kinetic-altered phenotypes were reverted to WT when the relative abundances of PETE2 or PETE1 were increased by overexpression.

In order to correlate the characteristics of photosynthetic electron flow of pete1 and pete2 mutant plants with their plastocyanin pool sizes and composition, thylakoid lumen samples isolated from WT and mutant leaves were fractionated by isoelectric focusing (IEF) followed by SDS polyacrylamide (2D-PAGE), and quantified by the difference gel electrophoresis (DIGE) technique (Figure 6A and 6B; Supplemental Figure 1). N-terminal sequencing and MALDI-TOF analysis allowed to assign four major spots to the two WT plastocyanin isoforms, with isoelectric points around pH 3 and molecular weights ranging between 15 and 10 kDa. Spots 1, 2, and 4 corresponded to PETE2 and spot 3 to PETE1 (Figure 6A). As expected, in pete2, the PETE1 isoform was the major form present and, in pete1, the PETE2 isoform predominated. No post-translational modifications of PETE1 and PETE2 could be detected by MALDI-TOF analysis and the molecular weights of the different spots do not support the presence of multiple plastocyanin aggregates.

Quantification of the plastocyanin spots revealed that, in WT leaves, the relative level of the two plastocyanin isoforms was similar to the PETE1/PETE2 RNA ratio, indicating that a good correlation between transcript and protein amounts exists (Figure 6B). As a matter of fact, in pete2 thylakoids, the plastocyanin content was reduced to 6% of WT level, whereas, in pete1, a reduction of 20–45% was observed. The plastocyanin-to-PSI ratio can also be estimated *in vivo* by measuring the absorption changes associated with the

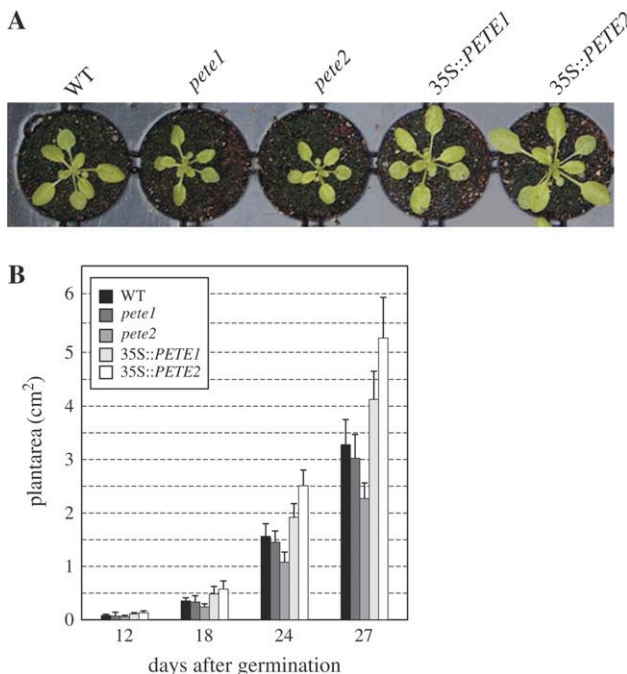


Figure 3. Growth Phenotypes of Mutant (pete1 and pete2), Over-expressor (35S::PETE1 and 35S::PETE2) and WT Plants.

(A) Four-week-old plants propagated in growth chamber.  
(B) Total leaf area measured at different times (in days) after germination. Average values for 50 plants of each genotype are reported. Bars indicate standard deviations.

Table 1. Light-Dependent Electron Transport Rate (ETR) in Leaves of WT, Mutants (pete1 and pete2), and Overexpressors (35S::PETE1 and 35S::PETE2).

PPFD ( $\text{1mol m}^{-2} \text{s}^{-1}$ )	WT	pete1	pete2	35S::PETE1	35S::PETE2
60	19.40 $\pm$ 0.09	19.15 $\pm$ 0.13	17.89 $\pm$ 0.05	19.53 $\pm$ 0.08	19.68 $\pm$ 0.11
150	37.82 $\pm$ 0.11	36.54 $\pm$ 0.08	33.39 $\pm$ 0.08	38.43 $\pm$ 0.06	37.8 $\pm$ 0.05
300	54.18 $\pm$ 0.09	54.18 $\pm$ 0.12	41.58 $\pm$ 0.07	54.18 $\pm$ 0.09	55.44 $\pm$ 0.06
600	70.56 $\pm$ 0.13	68.65 $\pm$ 0.18	55.44 $\pm$ 0.17	70.56 $\pm$ 0.19	73.08 $\pm$ 0.23

PPFD, photosynthetic photon flux density; ETR unit:  $\text{1mol m}^{-2} \text{s}^{-1}$ .

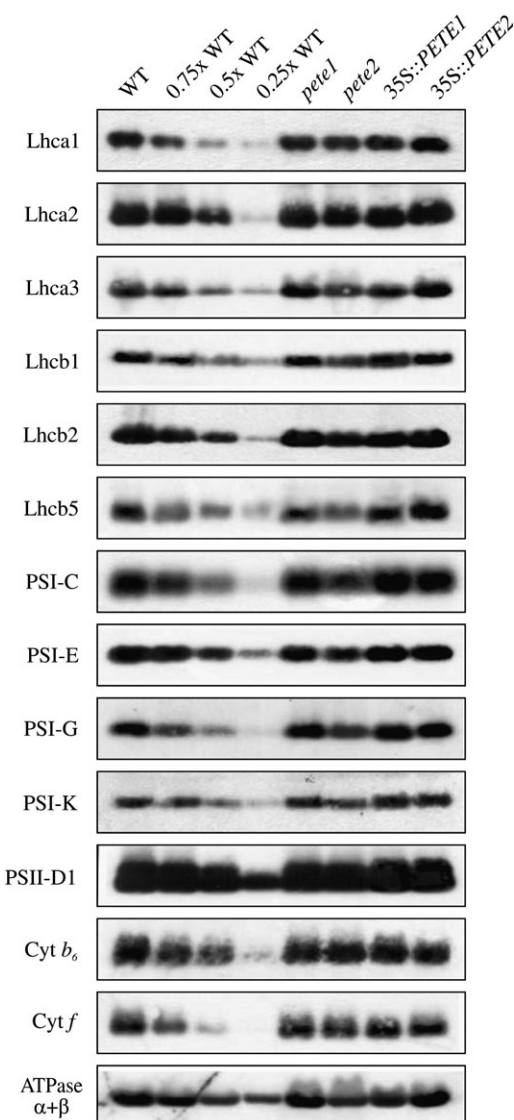


**Figure 4. Protein Composition of Thylakoid Membranes.** Thylakoid proteins obtained from identical amounts (fresh weight) of light-adapted WT, mutant (pete1 and pete2), and overexpressor (35S::PETE1 and 35S::PETE2) leaves were fractionated by SDS-PAGE. Decreasing levels of WT thylakoid proteins were loaded in the lanes marked 0.75xWT, 0.5xWT, and 0.25xWT and filters were probed with antibodies specific for the proteins indicated on the left. The results shown are representative of those obtained in three independent experiments.

oxidation of plastocyanin and  $P_{700}^+$  (Seigneurin-Berny et al., 2006). This approach revealed an overall trend for the different genotypes that was very similar to the one found by 2D-PAGE: a significant decrease in plastocyanin content in pete2 (to 15% of WT levels) and slight decrease in pete1 (80% of WT).

Taking this analysis and the phenotypic characterization of plastocyanin mutants together, the data imply that even drastic reductions of the plastocyanin pool size—although altering the electron flow between Cyt  $b_6/f$  and PSI, as seen in pete2

**Table 2. Amounts of Representative Thylakoid Proteins in Light-Adapted Plastocyanin Mutants (pete1 and pete2) and Overexpressors (35S::PETE1 and 35S::PETE2).**

Protein	pete1	pete2	35S::PETE1	35S::PETE2
Lhca1	100	92	100	100
Lhca2	100	69	100	100
Lhca3	100	86	94	100
Lhcb1	100	73	100	97
Lhcb2	100	88	93	100
Lhcb5	89	73	94	100
PSI-C	100	71	100	100
PSI-E	100	69	100	100
PSI-G	100	81	100	100
PSI-K	100	71	100	100
PSII-D1	100	95	100	100
Cyt $b_6$	100	100	100	100
Cyt f	100	96	100	100
ATPase (α+β)	100	61	72	100

Average values were derived from three independent Western analyses (as in Figure 4). Values are expressed as percentages of WT protein levels. Standard deviations were less than 5%.

plants—limit photosynthetic performance and growth only marginally under optimal growth conditions. In agreement with that, pete1 plants with about 60–80% of WT plastocyanin levels showed a WT-like phenotype, indicating that a large excess of plastocyanin is present in the thylakoid lumen of *Arabidopsis*.

#### Plastocyanin Isoforms Play a Redundant Role in Thylakoid Electron Transport

The great similarity in sequence between the two mature plastocyanin proteins suggests that PETE1 and PETE2 have redundant functions. To investigate this aspect further, lines expressing comparable levels of either PETE1 or PETE2 RNA, in the absence of the other transcript, were obtained by introducing into the pete1 pete2 double mutant background (Weigel et al., 2003) a PETE1 or PETE2 gene under the transcriptional control of the 35S promoter of Cauliflower Mosaic Virus. N-terminal sequencing and MALDI-TOF analysis, together with the quantification of plastocyanin spots, indeed, confirmed that the two overexpressors contained similar amounts of only one plastocyanin isoform each, both slightly higher than WT levels (Figure 6A and 6B). Similar results were also obtained when the plastocyanin-to-PSI ratio was estimated *in vivo* (see above), revealing an almost WT or somewhat larger amount of plastocyanin in the two overexpressors (95 and 137% of WT in 35S::PETE2 and 35S::PETE1, respectively). The increased dosage of either PETE1 (35S::PETE1) or PETE2 (35S::PETE2) in pete1 pete2 resulted in the production of WT-like plants. The effects of pete1 pete2 on thylakoid protein accumulation (Figure 4 and Table 2), leaf coloration (Figure 3A), and pigment content (data not shown) were fully

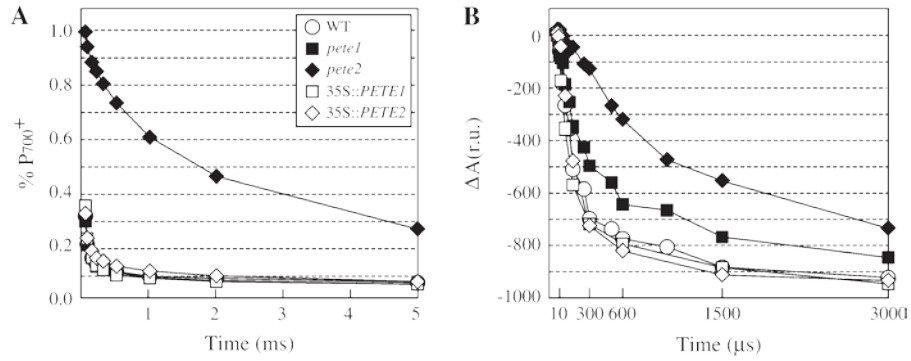


Figure 5. Measurements of Linear Electron Flow in Plastocyanin Mutant (pete1 and pete2), Overexpressor (35S::PETE1 and 35S::PETE2), and WT Leaves.

Six independent experiments on different biological samples were performed, and representative results are shown.

(A) The reduction kinetics of  $P_{700}^+$  following a single turnover actinic flash. A laser flash of 5 ns duration was applied at  $t = 0$  and the absorption changes associated with the reduction of the photo-oxidized  $P_{700}^+$  were followed. Data were normalized to the pete2 maximum value. WT, pete1, and overexpressor lines were characterized by an unresolved fast-phase (, 100 1s) accounting for about 60% of the absorption decay and a slow phase developing over 5 ms. The pete2 mutant was characterized by a prominent slow phase with a half-life of 1 ms.

(B) Kinetics of Cyt f oxidation following a single turnover actinic flash. A laser flash of 5 ns duration was applied at  $t = 0$  and the absorption changes associated with the oxidation of Cyt f monitored at 554 nm. In WT and overexpressor lines, the half-life of the fast-phase was about 100 1s, accounting for 75% of the absorption decay. The slow-phase (25%) had a half-life of about 1 ms. In pete1 and pete2, the amplitude of the slow-phase was increased by between 25 and 45%, and between 85 and 95%, respectively. Standard deviations were below 5% for the WT, pete2, and overexpressor lines. The standard deviation of the amplitude of the slow phase was larger in the pete1 mutant; its relative amplitude varied between 25 and 45%.

reversed in the PETE1 and PETE2 overexpressors. Interestingly, the 35S::PETE2 and, to a lesser extent, the 35S::PETE1 plants showed an increase in size, as indicated by measurements of leaf area (Figure 3A and 3B) and rosette dry-weights (data not shown); this effect became particularly evident after the first 3 weeks of growth. Measurements of photosynthetic electron flow were also carried out on the overexpressor lines. The  $U_{II}$  parameter at  $80 \text{ } \mu\text{mol m}^{-2} \text{ s}^{-1}$  of actinic light was identical among the different genotypes (WT:  $0.76 \pm 0.01$ ; 35S::PETE1:  $0.76 \pm 0.01$ ; 35S::PETE2:  $0.77 \pm 0.02$ ). Identical rates of linear electron transport were also observed (Table 1). Additionally, as mentioned above, both 35S::PETE1 and 35S::PETE2 overexpressors showed a WT-like behavior with respect to  $P_{700}^+$  reduction and Cyt f oxidation rates (Figure 5), indicating that the decreased rate of  $P_{700}^+$  reduction and Cyt f oxidation stems from the reduced plastocyanin content, namely diminished fraction of PSI with pre-bound plastocyanin.

Taking these analyses together, the data imply that the two plastocyanin isoforms are functionally equivalent, as predictable from the high sequence homology.

#### Plastocyanin and Cyt $c_{6A}$ have Distinct Roles in the Thylakoid Lumen

The limited change in photosynthetic performance seen in pete2 plants suggests that plastocyanin is normally present in large excess relative to the requirements for efficient electron transfer under optimal growth conditions. Therefore, in light of the proposal of Schlarb-Ridley et al. (2006) that plastocyanin and Cyt  $c_{6A}$  might cooperate in the thylakoid lumen,

we considered the possibility that the excess plastocyanin accepts electrons from Cyt  $c_{6A}$ . Because the physical interaction of the two proteins is a prerequisite for electron transfer from Cyt  $c_{6A}$  to plastocyanin, we used yeast two-hybrid experiments to test whether Cyt  $c_{6A}$  and plastocyanin can interact physically in vivo. When Cyt  $c_{6A}$  fused to the GAL4 activation domain (Cyt  $c_{6A}^{AD}$ ) was co-expressed with the GAL4 DNA-binding domain fused to either PETE1 or PETE2 (PETE1<sup>BD</sup>, PETE2<sup>BD</sup>), yeast cells did not grow on selective medium lacking either histidine or adenine, indicating that Cyt  $c_{6A}$  does not interact with either of the two plastocyanin isoforms (Supplemental Figure 2A). Furthermore, no interaction between PETE1 and PETE2 (PETE2<sup>BD</sup> + PETE1<sup>AD</sup>) could be observed. Interestingly, yeast cells grew very robustly on selective medium when Cyt  $c_{6A}^{AD}$  was co-expressed with the GAL4 DNA-binding domain (BD) fused to a second Cyt  $c_{6A}$  molecule (Cyt  $c_{6A}^{BD}$ ), suggesting that Cyt  $c_{6A}$  is able to form homodimers. The interaction persisted even when a mutated form of Cyt  $c_{6A}$ , in which the two conserved cysteines were replaced by two serines (Cyt  $c_{6A}m$ ), was fused to the GAL4 DNA-binding domain (Cyt  $c_{6A}m^{BD}$ ), implying that formation of Cyt  $c_{6A}$  homodimers is not dependent on the formation of disulphide bridges. Whether a ternary complex made up of Cyt  $c_{6A}$  homodimers and either plastocyanin type could form was also tested using a yeast ternary-trap assay (Egea-Cortines et al., 1999) (Supplemental Figure 2B). To this end, the Cyt  $c_{6A}^{AD}$  fusion protein was co-expressed with a Cyt  $c_{6A}$  carrying a nuclear localization signal (Cyt  $c_{6A}^{TFT}$ ), together with either PETE1<sup>BD</sup> or PETE2<sup>BD</sup>. In all cases, yeast cells were unable to grow on selective medium, suggesting the

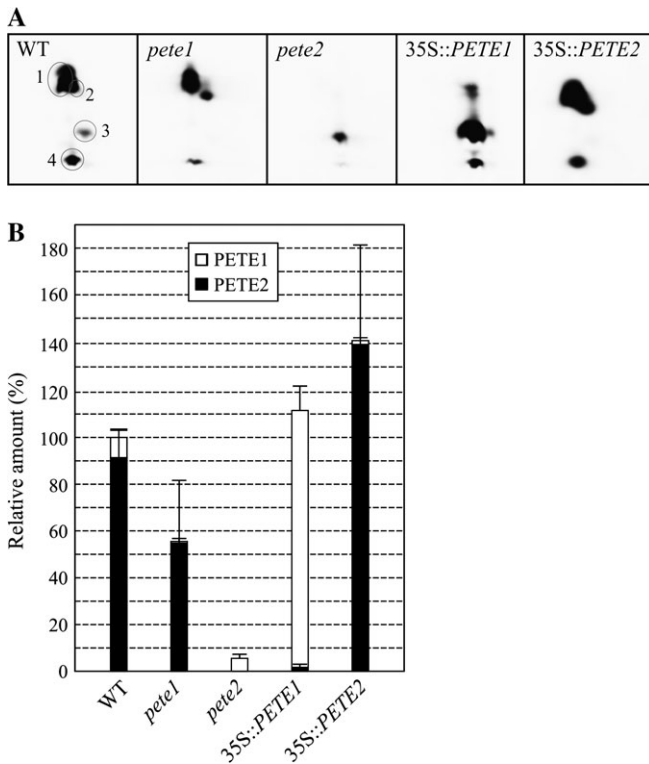


Figure 6. Plastocyanin Content in Mutant (pete1 and pete2), Over-expressor (35S::PETE1 and 35S::PETE2), and WT Plants.

After isolation of the thylakoid lumen fraction, proteins were fractionated according to the isoelectric point in the first dimension and by SDS-PAGE in the second dimension.

(A) Details of 2D-gels for the different genotypes (see Supplemental Figure 1 for a representative entire gel image). Spots were assigned to plastocyanin isoforms by MS analysis: spots 1, 2, and 4 (blue circles) contain PETE2; spot 3 contains PETE1 (green circle).

(B) Quantification of plastocyanin spots shown in (A).

Note that the small amounts of PETE1 in pete1 and in 35S::PETE2 lines, as well as of PETE2 in 35S::PETE2 lines, are due to residual contaminations.

absence of any interaction between Cyt  $c_{6A}$  and the plastocyanin isoforms, even under conditions that are permissive for the formation of higher-order complexes.

A putative interaction between Cyt  $c_{6A}$  and plastocyanin was also tested at the genetic level. Based on the hypothesis of Schlarb-Ridley et al. (2006), Cyt  $c_{6A}$  knockout plants with reduced plastocyanin content should be markedly affected in thylakoid function and may even be lethal. To test this hypothesis, a Cyt  $c_{6A}$  knockout line (atc6-1) (Figure 7 and Supplemental Figure 3; see also Methods) was crossed with pete1 or pete2 plants and double mutants were selected in the F2 progenies. Interestingly, the atc6-1 pete1 and atc6-1 pete2 double mutants and the corresponding pete single mutants exhibited identical phenotypes, in terms of both growth rate and photosynthetic performance (Figure 7). Indeed, even under high-light conditions, the pete2 and atc6-1 pete2 mutants showed an identical level of photosensitivity.

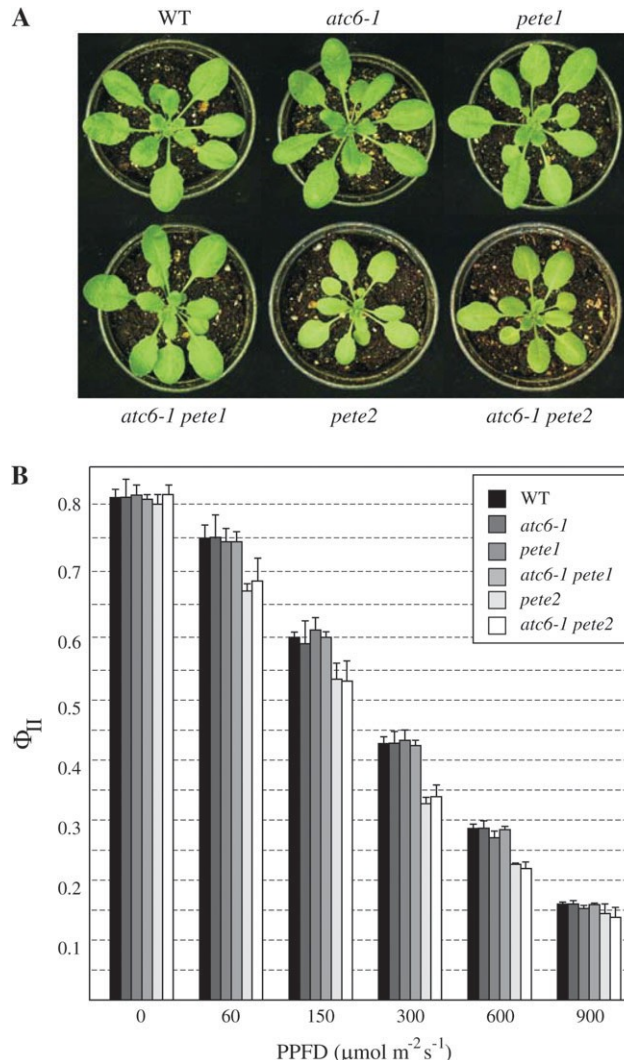


Figure 7. Phenotypes of atc6-1, pete1, pete2, atc6-1 pete1, atc6-1 pete2, and WT Plants.

(A) Four-week-old plants grown in a growth chamber.

(B) Light-dependent photosynthetic performance, measured as effective quantum yield of PSII ( $\Phi_{II}$ ), of plants grown as in (A).

#### Increased Availability of Cu Exacerbates the pete2 Phenotype

To study the effects of variations in plastocyanin amounts on Cu contents, we analyzed the ion concentrations in thylakoids isolated from WT, pete mutants, and overexpressors. Reductions of about 30 and 85% in Cu content were detected in pete1 and pete2 mutants, respectively, implying a good correlation between plastocyanin content and thylakoid Cu concentration (Table 3).

Given the important role of plastocyanin as a Cu sink (Ramshaw et al., 1973; Märschner, 2002), we tested the effects of varying Cu supply on the growth behavior of plastocyanin mutants and overexpressors. Plants were cultured on solid agar medium with different concentrations of  $\text{CuSO}_4$ , and leaf

Table 3. Cu Contents in Thylakoids of WT, Mutants (pete1 and pete2), and Overexpressors (35S::PETE1 and 35S::PETE2).

	WT	pete1	pete2	35S:: PETE1	35S:: PETE2
Thylakoids	17.48	6 1.4	12.41	6 1.27	2.33 6 0.51

Values indicate amounts of Cu expressed as mg g<sup>-1</sup> Mg. The data are averages (6 SD) of three independent measurements.

areas of 2-week-old seedlings were measured as an indicator of growth (Supplemental Figure 4). At 0.025, 0.1, and 10 1M CuSO<sub>4</sub>, no major differences in size were observed between the genotypes tested. However, at 25 1M CuSO<sub>4</sub>, pete2 plants showed a marked reduction in growth (Supplemental Figure 4). Concomitantly, an evident decrease in photosynthetic performance was also observed in pete2, indicating that the reduced plastocyanin pool size decreases the threshold level for Cu toxicity.

## DISCUSSION

Variations in plastocyanin levels have been repeatedly reported to coincide with variations of photosynthetic electron transport activity (Krueger et al., 1984; Burkey, 1993, 1994; Burkey et al., 1996; Schöttler et al., 2004), prompting the conclusion that the plastocyanin pool size is limiting for thylakoid electron transport. On the contrary, our analysis shows that the plastocyanin content can be significantly decreased without pronounced changes in the overall photosynthetic activity, suggesting that—at least in *Arabidopsis* WT plants under optimal growth conditions—plastocyanin is present in large excess. An up to 10-fold decrease in the plastocyanin content is apparently of little consequence for overall photosynthetic activity and pete1 plants with 60–80% of WT plastocyanin levels are hardly changed in growth rate and photosynthesis efficiency. This indicates that the plastocyanin-to-PSI ratio of 2–3 observed in spinach (Graan and Ort, 1984; Haehnel et al., 1989) or green algae (Delosme, 1991) is not a strict prerequisite for efficient photosynthesis, although it certainly promotes saturation of the PSI binding site for plastocyanin and, therefore, rapid reduction of P<sub>700</sub><sup>+</sup>. Similarly, *Synechocystis* mutants without cytochrome c<sub>6</sub> (Cyt c<sub>6</sub>) and with heavily down-regulated plastocyanin expression grow photoautotrophically and maintain rapid steady-state photosynthetic electron transport rates (Zhang et al., 1994). Taken together, it appears likely that limited amounts of plastocyanin, in plants grown under optimal conditions, are still capable of an efficient electron transport.

This prompts the question of why there is so much plastocyanin in the thylakoid lumen of *Arabidopsis*. One possible explanation is that a significant excess of plastocyanin relative to PSI ensures saturation of the plastocyanin docking site, keeping the lifetime of P<sub>700</sub><sup>+</sup> short by promoting its fast reduction when plastocyanin is pre-bound to PSI. Such a requirement

has been put forward on the basis of the increased photosensitivity observed in mutants lacking the PSI-F subunit, which is involved in the docking of plastocyanin in *C. reinhardtii* (Hippler et al., 2000) and *A. thaliana* (Haldrup et al., 2000). Interestingly, pete2 plants that also lack pre-bound plastocyanin showed a similar photosensitivity, implying that the large amount of plastocyanin might have an essential role in protecting higher plants from photooxidative damages. The alternative explanation—that plastocyanin interacts physically with Cyt c<sub>6A</sub> to function as a redox buffer in the thylakoid lumen (Schlarb-Ridley et al., 2006)—finds no support from our yeast analyses, although the existence of a transient weak interaction that escapes detection by the yeast two-hybrid assay, cannot be excluded. However, one tenet of the hypothesis of Schlarb-Ridley et al. (2006) needs to be revised: in contrast to previous reports (Gupta et al., 2002), in our hands, the lack of Cyt c<sub>6A</sub> expression (in the atc6-1 mutant) in combination with reduced plastocyanin expression does not lead to a synthetic phenotype, thus making a functional interaction of the two luminal proteins unlikely.

The involvement of plastocyanin in Cu homeostasis has been also suggested before, because this soluble electron carrier chelates around 50% of Cu in photosynthetic cells (Ramshaw et al., 1973). Although a marked reduction in Cu content could be detected in thylakoid membranes isolated from pete1 and pete2 leaves, similarly to the decrease in thylakoid Cu reported for the paa1 and paa2 mutants (Shikanai et al., 2003; Abdel-Ghany et al., 2005), it is unlikely that plastocyanin acts as a metallothionein mediating Cu tolerance in flowering plants (Zhou and Goldsborough, 1995). Accordingly, the plastocyanin overexpressor lines did not exhibit increased resistance to Cu stress, and presumably the reduced plastocyanin content rendered the pete plants more susceptible to oxidative stress when grown under high-Cu conditions. Alternatively, excess levels of plastocyanin might become necessary under certain stress conditions affecting the mobility of plastocyanin. For instance, in *Chlamydomonas* under hyper-osmotic shock, the reduced luminal space hinders the movement of docking to PSI of plastocyanin (Cruz et al., 2001). Although land plants might be rarely exposed to such extreme stress conditions, the high levels of plastocyanin might represent a pre-adaptation to such conditions, ensuring an optimal lateral diffusion under chilling temperatures or drought stress.

In contrast to algae and cyanobacteria, *Arabidopsis*, together with many other flowering plants and the moss *Physcomitrella*, expresses more than one isoform of plastocyanin. In poplar, the amino acid substitutions that distinguish the two plastocyanin isoforms are associated with differences in electrostatic properties and influence protein stability (Shosheva et al., 2004, 2005); yet, the characterization of the consequences on the function of plastocyanin, namely the transfer of electrons between PSI and Cyt f, is still lacking. In our analysis, a direct correlation between photosynthetic performance and the amount of plastocyanin available was found in *A. thaliana*, regardless of the isoform analyzed. This suggests that, *in vivo*,

the two plastocyanin isoforms have redundant function. It is also reminiscent of previous studies of the D (Ihnatowicz et al., 2004) and E (Ihnatowicz et al., 2007) subunits of PSI: each of these is encoded by two functional nuclear genes, and, in each case, the two isoforms have identical functions. However, the presence of two functional plastocyanin-encoding genes raises the question of why these genes are duplicated in the nuclear genomes of several flowering plants. One possible explanation is that PETE gene duplications have been positively selected in different land plant species independently, because these organisms—in contrast to algae and cyanobacteria (Merchant et al., 2006)—lack Cyt c<sub>6</sub> as an alternative electron transporter and are more subject to fluctuating metal ion concentrations than other organisms, due to their sessile nature. This might have made it necessary to regulate the expression of plastocyanin in a more flexible manner, with the aim to guarantee an efficient electron transport rate especially under extreme stress conditions. That is in agreement with the highly variable abundance of plastocyanin observed under the different environmental conditions (Burkey, 1993; Schöttler et al., 2004).

One unexpected finding was that overexpression of either PETE1 or PETE2 results in an increase in size and in dry weight of leaves, implying an enhanced capacity for biomass production. However, the improved growth rate of 35S::PETE1 and 35S::PETE2 lines could not be ascribed to an increase in photosynthetic capacity; accumulation of photosynthetic proteins and chlorophyll fluorescence parameters were similar to WT. Chida et al. (2007) have recently reported a similar enhancement of plant growth upon overexpression of an algal Cyt c<sub>6</sub> in *A. thaliana*. This overexpressor, however, had a higher capacity for CO<sub>2</sub> fixation and improved photosynthetic electron flow. In both the study by Chida et al. (2007) and our analysis, a clear explanation for the increase in biomass production remains elusive, particularly in light of the large excess of plastocyanin already present in WT *Arabidopsis* thylakoids.

## METHODS

### Plant Lines, Propagation, and Growth Measurements

The pete1 and pete2 mutants were identified among a collection of *A. thaliana* (ecotype Col-0) lines that had been mutagenized by random insertion of the En1 transposon from maize (Weigel et al., 2003). Stable null alleles were obtained as previously described (Weigel et al., 2003). The atc6-1 mutant, corresponding to the line Salk\_011266 (ecotype Col-0), was identified by screening the insertion flanking database SIGnAL (<http://signal.salk.edu/cgi-bin/tdnaexpress>). Details of T-DNA insertion and the primers used for segregation analysis are given in Supplemental Figure 3. The atc6-1 pete1 and atc6-1 pete2 double mutants were generated by crossing the corresponding single mutants and identifying homozygous F2 plants by PCR. The overexpressing lines 35S::PETE1 and 35S::PETE2 were generated by ligating the PETE1 and PETE2

cDNAs, respectively, into the plant expression vector pJAN33, placing them under the control of the Cauliflower Mosaic Virus 35S promoter. Flowers from pete1/pete1 PETE2/pete2 plants were transformed according to Clough and Bent (1998) and seeds were collected after 3 weeks. Forty-five and 51 independent transgenic plants for 35S::PETE1 and 35S::PETE2, respectively, were selected on the basis of their kanamycin resistance, and pete1 pete2 double mutants carrying the corresponding transgene were identified by PCR. Overexpression of the transgenes was confirmed by Northern analysis and RT-PCR, and plants were phenotypically analyzed by measuring growth and chlorophyll fluorescence as described (Leister et al., 1999; Pesaresi et al., 2001).

All genotypes were grown on Minitray soil (Gebr. Patzer, Sinntal-Jossa, Germany) in a growth chamber (day period of 11 h at 20°C, PPFD = 80 1mol m<sup>-2</sup> s<sup>-1</sup>; night period of 13 h at 15°C). Osmocote Plus fertilizer (15% N, 11% P<sub>2</sub>O<sub>5</sub>, 13% K<sub>2</sub>O, and 2% MgO; Scotts Deutschland, Nordhorn, Germany) was used according to the manufacturer's instructions. For growth on agar medium, seeds were surface-sterilized and sown on agar plates containing MS medium including 1% sucrose (Sigma-Aldrich, St Louis, MO). The medium was supplemented with different concentrations of CuSO<sub>4</sub> (0.025 1M; 0.1 1M; 10 1M; 25 1M) or with the chelator cuprizone (Sigma #C9012) as indicated. To induce high-light stress, 3-week-old plants, grown on soil as above, were exposed to a light flux of 800 1mol m<sup>-2</sup> s<sup>-1</sup> (during the daily 11-h photoperiod) for 1 week. All the analyses, unless stated elsewhere, were performed on light-adapted plants at the eight-leaf rosette stage.

### Analysis of Nucleic Acids and their Sequences

*Arabidopsis* DNA was isolated as described by Liu et al. (1995). Total RNA was extracted from fresh tissue using the RNeasy plant system (Qiagen, Hilden, Germany). For QRT-PCR of PETE1 and PETE2, first-strand cDNA was synthesized using the SuperScript preamplification system (Invitrogen, Karlsruhe, Germany), and a <sup>33</sup>P-labeled PETE gene-specific sense primer was used with unlabeled antisense primer (PETE-sense: 5'-MATCCCWTCTTCACCGGCCT-3'; PETE-antisense: (5'-CACRAT-CTTCTCTCCTTTAGC-3') to amplify cDNA by PCR for 25 cycles. In the same reaction, a <sup>33</sup>P-labeled ACTIN1 gene-specific sense primer was used with unlabeled antisense primer to check for equal loading (Actin1-sense: 5'-TTCACCACACAGCAGAGC-3'; Actin1-antisense: 5'-ACCTCAGGACAACCGGAATCG-3'). The PCR products were then separated on a 4.5% (w/v) polyacrylamide gel. Signals were quantified using the Storm 860 PhosphorImager (Molecular Dynamics) and the program Image Quant for Macintosh (version 1.2; Molecular Dynamics).

Sequence data were analyzed with the Winsconsin Package Version 10.0 from the Genetic Computer Group, Madison, Winsconsin (GCG; Devereux et al., 1984) and amino acid sequences were aligned using CLUSTALW ([www.ebi.ac.uk/clustalw](http://www.ebi.ac.uk/clustalw); Thompson et al., 1994).

## Protein Gel-Blot Analyses and Two-Dimensional PAGE

For immunoblot analyses, leaves were harvested in the middle of the light period and thylakoids were prepared as described by Bassi et al. (1985). Thylakoid proteins obtained from identical amounts (fresh weights) of WT, mutant, and overexpressor leaves were fractionated by electrophoresis on a SDS-PAGE gradient gel (10–16% acrylamide) as described by Schägger and von Jagow (1987) and transferred to Immobilon-P membranes (Millipore). Replicate filters were incubated with antibodies specific for the antenna complex of PSI (Lhca1-3), PSI-C, PSI-E, PSI-G, PSI-K, Cyt b<sub>6</sub>, Cyt f, the antenna complex of PSII (Lhcb1-2, Lhcb5), PSII-D1, and the ATPase a + b subunits. Signals were detected using the Enhanced Chemiluminescence Western Blotting Kit (Amersham Biosciences, Sunnyvale, CA). Densitometric analyses of immunoblot signals were performed using lumi Analyst 3.0 (Boehringer Mannheim).

For plastocyanin quantification, the thylakoid lumen fraction was isolated essentially as in Kieselbach et al. (1998). Proteins were concentrated using Microsep<sup>TM</sup> Centrifugal Devices 3K (PALL Life Sciences), and protein quantification was carried out according to Bradford (1976) using bovine serum albumin as standard. Subsequently, lumen proteins (150  $\mu$ g) were precipitated with ice-cold 100% acetone, solubilized and labeled according to GE healthcare instruction manual for DIGE (CyDye DIGE Fluors minimal dyes for Ettan DIGE) with the exception that the end concentration in the solubilization mixture was 7 M urea, 2 M thiourea, 5 mM Tris, 0.2% SDS and 4% CHAPS. Samples were separated by isoelectric focusing (IEF) in the pH range between 3.0 and 5.6 on 24-cm strips (GE healthcare). An Ettan IPGphor II was used for strip rehydration (12 h), and the separation was completed at a constant voltage of 8000 V for  $\geq 90\,000$  Vh. Each strip was then equilibrated for 15 min with gentle rolling in 25 ml of equilibration solution (50 mM Tris-Cl, pH 8.8, 6 M urea, 30% glycerol, 2% SDS) with 2% DTT and for 15 min in equilibration solution containing 4.5% iodoacetamide instead of the DTT. Fractionation in the second dimension was performed on denaturing SDS-PAGE gradient gels (12–20% acrylamide), cast in an EttanDaltsix caster using low fluorescence glass plates. Gels were run according to the EttanDaltsix user's manual (Ettan Daltsix Electrophoresis System, second-dimension gel electrophoresis 80–6492–49/Rev. B0/07–03, Amersham Biosciences) at 14 mA and 20°C.

## Protein Detection and Image Analysis

The gels were scanned with a Typhoon<sup>TM</sup> 9410 (Amersham Biosciences) Variable Mode Imager at 100  $\mu$ m resolution with PMTs set in the 490–550 V range. Image edges were cropped using ImageQuant<sup>TM</sup> V5.2 (Amersham Biosciences) and the images were analyzed with DeCyder<sup>TM</sup> V5.0 software (Amersham Biosciences). The batch processor was run with an estimated spot number of 1200. Detailed descriptions of the DeCyder<sup>TM</sup> are given by Alban et al. (2003) and in the Ettan DIGE User's Manual (18–1164–40 Amersham Biosciences). After scanning, the gels were fixed with 40% ethanol and 10% acetic acid, and stained with a filtered and boiled solution of

0.025% R-250 Coomassie Blue in 10% acetic acid for 15 min. The gels were then destained with 10% acetic acid.

## N-terminal Sequencing

Amino-terminal microsequencing was carried out with a Procise sequencer (Applied Biosystems). Proteins from 1D and 2D PAGE were transferred to a polyvinylidene difluoride (PVDF) membrane and sequenced essentially as described (Matsudaira, 1987).

## MALDI-TOF Analysis

MALDI-TOF analysis of proteins digested in-gel was carried out with the Vouager-DE<sup>TM</sup> STR Bio Spectrometry<sup>TM</sup> Workstation from PerSpective Biosystem. In-gel digestions were performed using a combination of sequencing-grade modified chymotrypsin (Promega) and trypsin, and then analyzed as described by Shevchenko et al. (1996). Database searches were performed with the MS BioTools software (Bruker) using the Mascott search engine ([www.matrixscience.com](http://www.matrixscience.com)). Proteins that could not be identified from fingerprint spectra were confirmed by a post-source decay analysis of single peptides.

## Spectroscopic Analyses

In-vivo chlorophyll a fluorescence of single leaves was measured using the PAM 101/103 fluorometer (Walz, Effeltrich, Germany). Pulses (800 ms) of white light ( $6000\,1\text{mol m}^{-2}\text{ s}^{-1}$ ) were used to determine the maximum fluorescence ( $F_M$ ). A 15-min illumination with actinic light ( $80\,1\text{mol m}^{-2}\text{ s}^{-1}$ ) served to drive electron transport between PSII and PSI before measuring  $U_{II}$ , ETR (Genty et al., 1989) and qP. For  $U_{II}$  light-curves, plants were adapted for 15 min to each of the light intensities, ranging from 60 to  $900\,1\text{mol m}^{-2}\text{ s}^{-1}$ .

Spectrophotometric measurements were made on a flash spectrophotometer (JTS 10, Biologic, France) as described previously (Joliot and Joliot, 2005). Transient changes in P<sub>700</sub> oxidation were determined using an 810-nm broadband LED source (30 nm). RG780 filters were used to protect the photodiodes from actinic light. When continuous light was used, the actinic FRL was provided by a far-red LED ( $k_{\text{max}} = 720$  nm) filtered through three Wratten filters 55 that block wavelengths below 700 nm. Green light was provided by an inbuilt array of LEDs ( $k_{\text{max}} = 530$  nm). The fast P<sub>700</sub><sup>+</sup> reduction kinetics (see Figure 5) were measured with the same set-up using a dye laser to provide the actinic flash.

Changes in Cyt f absorption were measured with a set-up described in Beal et al. (1999). Actinic flashes were provided by a dye laser at 690 nm, while detecting flashes were provided by an optical parametric oscillator (OPO) pumped by a Nd:Yag laser. The Cyt f redox changes were obtained as the difference between the absorption at 554 nm and a baseline drawn between 545 and 573 nm.

The plastocyanin-to-PSI ratio was assessed by measuring the absorption changes at 810 and 870 nm induced by a far-red illumination (720 nm), to fully oxidized both P<sub>700</sub> and the electron donors, including plastocyanin. The absorption changes

at 810 nm were corrected for the plastocyanin contribution to assess the absorption changes resulting specifically from  $P_{700}^+$  oxidation, by computing the difference ( $DI/I_{810\text{nm}} - 0.8 DI/I_{870\text{nm}}$ ). Conversely, the absorption changes at 870 nm were corrected for the contribution of  $P_{700}^+$  to assess the absorption changes associated with the oxidation of plastocyanin, by computing the difference ( $DI/I_{870\text{nm}} - 0.25 DI/I_{810\text{nm}}$ ).

#### Yeast Two-Hybrid and Ternary-Trap Assays

YPAD, SD, and appropriate dropout media have been described previously (Sherman, 1991). The yeast two-hybrid and the ternary-trap assays were performed using the yeast strain AH109 supplied by Clontech (Palo Alto, CA) (James et al., 1996). The pGBTKT7 vector (Clontech), carrying the GAL4 DNA-binding domain, was used to express the bait proteins, whereas the pGADT7 vector (Harper et al., 1993), carrying the GAL4 activation domain, was used to express the prey proteins. For the ternary-trap test, the vector pTFT1 (Egea-Cortines et al., 1999) was employed. Two-hybrid protein interactions were evaluated by growing the yeast colonies at 28°C on media lacking either histidine or adenine and supplemented with different amounts of 3-amino-1,2,4-triazole (3-AT). Ternary-trap assays were evaluated on media containing 3-AT but lacking histidine.

#### Cu and Mg Quantification

Thylakoids obtained from soil-grown WT, mutants, and over-expressors were oven-dried for 2 d at 60°C. Afterwards, the material was subjected to mineralization for 2 d in 65% nitric acid at 100°C. After mineralization, Cu and Mg contents were quantified by means of ICP-MS analysis (EPA 200.8).

## SUPPLEMENTARY DATA

Supplementary Data are available at Molecular Plant Online.

## FUNDING

This work was supported by the Deutsche Forschungsgemeinschaft (grants LE 1265/10 and SFB-TR1 TP B7 to D.L.) and the Swedish Research Council (grant FORMAS to W.S.P. and I.G.).

## ACKNOWLEDGMENTS

We thank Paul Hardy for critical comments on the manuscript. No conflict of interest declared.

## REFERENCES

Abdel-Ghany, S.E., Muller-Moule, P., Niyogi, K.K., Pilon, M., and Shikanai, T. (2005). Two P-type ATPases are required for copper delivery in *Arabidopsis thaliana* chloroplasts. *Plant Cell* 17, 1233–1251.

Alban, A., David, S.O., Bjorkesten, L., Andersson, C., Sloge, E., Lewis, S., and Currie, I. (2003). A novel experimental design for comparative two-dimensional gel analysis: two-dimensional difference gel electrophoresis incorporating a pooled internal standard. *Proteomics* 3, 36–44.

Bassi, R., dal Belin Peruffo, A., Barbato, R., and Ghisi, R. (1985). Differences in chlorophyll-protein complexes and composition of polypeptides between thylakoids from bundle sheaths and mesophyll cells in maize. *Eur. J. Biochem.* 146, 589–595.

Beal, D., Rappaport, F., and Joliot, P. (1999). A new high-sensitivity 10-ns time-resolution spectrophotometric technique adapted to *in vivo* analysis of the photosynthetic apparatus. *Review of Scientific Instruments* 70, 202–207.

Blanc, G., Hokamp, K., and Wolfe, K.H. (2003). A recent polyploidy superimposed on older large-scale duplications in the *Arabidopsis* genome. *Genome Res.* 13, 137–144.

Bradford, M.M. (1976). A rapid and sensitive method for the quantitation of microgram quantities of protein utilizing the principle of protein-dye binding. *Anal. Biochem.* 72, 248–254.

Briggs, L.M., Pecoraro, V.L., and McIntosh, L. (1990). Copper-induced expression, cloning, and regulatory studies of the plastocyanin gene from the cyanobacterium *Synechocystis* sp. PCC 6803. *Plant Mol. Biol.* 15, 633–642.

Buchanan, B.B., and Luan, S. (2005). Redox regulation in the chloroplast thylakoid lumen: a new frontier in photosynthesis research. *J. Exp. Bot.* 56, 1439–1447.

Burkey, K. (1993). Effect of growth irradiance on plastocyanin levels in barley. *Photosynth. Res.* 36, 103–110.

Burkey, K.O. (1994). Genetic variation of photosynthetic electron transport in barley: identification of plastocyanin as a potential limiting factor. *Plant Science* 98.

Burkey, K.O., Gizlice, Z., and Carter, T.E. (1996). Genetic variation in soybean photosynthetic electron transport capacity is related to plastocyanin concentration in the chloroplast. *Photosynth. Res.* 49, 141–149.

Chida, H., et al. (2007). Expression of the algal cytochrome  $c_6$  gene in *Arabidopsis* enhances photosynthesis and growth. *Plant Cell Physiol.* 48, 948–957.

Clough, S.J., and Bent, A.F. (1998). Floral dip: a simplified method for *Agrobacterium*-mediated transformation of *Arabidopsis thaliana*. *Plant J.* 16, 735–743.

Cruz, J.A., Salbilla, B.A., Kanazawa, A., and Kramer, D.M. (2001). Inhibition of plastocyanin to  $P_{700}^+$  electron transfer in *Chlamydomonas reinhardtii* by hyperosmotic stress. *Plant Physiol.* 127, 1167–1179.

Delosme, R. (1991). Electron transfer from cytochrome  $f$  to photosystem I in green algae. *Photosynth. Res.* 29, 45–54.

Devereux, J., Haeberli, P., and Smithies, O. (1984). A comprehensive set of sequence analysis programs for the VAX. *Nucleic Acids Res.* 12, 387–395.

Dimitrov, M.I., Donchev, A.A., and Egorov, T.A. (1990). Microheterogeneity of parsley plastocyanin. *FEBS Lett.* 265, 141–145.

Dimitrov, M.I., Donchev, A.A., and Egorov, T.A. (1993). Twin plastocyanin dimorphism in tobacco. *Biochim Biophys. Acta* 1203, 184–190.

Egea-Cortines, M., Saedler, H., and Sommer, H. (1999). Ternary complex formation between the MADS-box proteins SQUAMOSA,

DEFICIENS and GLOBOSA is involved in the control of floral architecture in *Antirrhinum majus*. *EMBO J* 18, 5370–5379.

Farah, J., Rappaport, F., Choquet, Y., Joliot, P., and Rochaix, J.D. (1995). Isolation of a psaF-deficient mutant of *Chlamydomonas reinhardtii*: efficient interaction of plastocyanin with the photosystem I reaction center is mediated by the PsaF subunit. *EMBO J* 14, 4976–4984.

Finazzi, G., Sommer, F., and Hippler, M. (2005). Release of oxidized plastocyanin from photosystem I limits electron transfer between photosystem I and cytochrome b6f complex in vivo. *Proc. Natl Acad. Sci. U S A* 102, 7031–7036.

Genty, B., Briantais, J.M., and Baker, N.R. (1989). The relationship between the quantum yield of photosynthetic electron transport and quenching of chlorophyll fluorescence. *Biochim. Biophys. Acta* 990, 87–92.

Gorman, D.S., and Levine, R.P. (1965). Cytochrome f and plastocyanin: their sequence in the photosynthetic electron transport chain of *Chlamydomonas reinhardtii*. *Proc. Natl Acad. Sci. U S A* 54, 1665–1669.

Graan, T., and Ort, D.R. (1984). Quantitation of the rapid electron donors to P700, the functional plastoquinone pool, and the ratio of the photosystems in spinach chloroplasts. *J. Biol. Chem.* 259, 14003–14010.

Gupta, R., He, Z., and Luan, S. (2002). Functional relationship of cytochrome c<sub>6</sub> and plastocyanin in *Arabidopsis*. *Nature* 417, 567–571.

Haehnel, W., Ratajczak, R., and Robenek, H. (1989). Lateral distribution and diffusion of plastocyanin in chloroplast thylakoids. *J. Cell Biol.* 108, 1397–1405.

Haehnel, W., Jansen, T., Gause, K., Klösgen, R.B., Stahl, B., Michl, D., Huvermann, B., Karas, M., and Herrmann, R.G. (1994). Electron transfer from plastocyanin to photosystem I. *EMBO J* 13, 1028–1038.

Haldrup, A., Simpson, D.J., and Scheller, H.V. (2000). Down-regulation of the PSI-F subunit of photosystem I (PSI) in *Arabidopsis thaliana*: the PSI-F subunit is essential for photoautotrophic growth and contributes to antenna function. *J. Biol. Chem.* 275, 31211–31218.

Harper, J.W., Adam, G.R., Wie, N., Keyomarsi, K., and Elledge, S.J. (1993). The p21 Cdk-interacting protein Cip1 is a potent inhibitor of G1 cyclin-dependent kinases. *Cell* 75, 805–816.

Hippler, M., Biehler, K., Krieger-Liszkay, A., van Dillewijn, J., and Rochaix, J.D. (2000). Limitation in electron transfer in photosystem I donor side mutants of *Chlamydomonas reinhardtii*: lethal photo-oxidative damage in high light is overcome in a suppressor strain deficient in the assembly of the light harvesting complex. *J. Biol. Chem.* 275, 5852–5859.

Ihnatowicz, A., Pesaresi, P., and Leister, D. (2007). The E subunit of photosystem I is not essential for linear electron flow and photoautotrophic growth in *Arabidopsis thaliana*. *Planta* 226, 889–895.

Ihnatowicz, A., Pesaresi, P., Varotto, C., Richly, E., Schneider, A., Jahns, P., Salamini, F., and Leister, D. (2004). Mutants for photosystem I subunit D of *Arabidopsis thaliana*: effects on photosynthesis, photosystem I stability and expression of nuclear genes for chloroplast functions. *Plant J* 37, 839–852.

James, P., Halladay, J., and Craig, E.A. (1996). Genomic libraries and a host strain designed for highly efficient two-hybrid selection in yeast. *Genetics* 144, 1425–1436.

Joliot, P., and Joliot, A. (2002). Cyclic electron transfer in plant leaf. *Proc. Natl Acad. Sci. U S A* 99, 10209–10214.

Joliot, P., and Joliot, A. (2005). Quantification of cyclic and linear flows in plants. *Proc. Natl Acad. Sci. U S A* 102, 4913–4918.

Katoh, S. (1960). A new copper protein from *Chlorella ellisoidea*. *Nature* 186, 533–534.

Kieselbach, T., Hagman, A., Andersson, B., and Schroder, W.P. (1998). The thylakoid lumen of chloroplasts. Isolation and characterization. *J. Biol. Chem.* 273, 6710–6716.

Kieselbach, T., Bystedt, M., Hynds, P., Robinson, C., and Schroder, W.P. (2000). A peroxidase homologue and novel plastocyanin located by proteomics to the *Arabidopsis* chloroplast thylakoid lumen. *FEBS Lett.* 480, 271–276.

Krueger, R.W., Randall, D.D., and Miles, D. (1984). Photosynthesis in tall fescue: V. Analysis of high PSI activity in a decaploid genotype. *Plant Physiol.* 76, 903–909.

Leister, D., Varotto, C., Pesaresi, P., Niwergall, A., and Salamini, F. (1999). Large-scale evaluation of plant growth in *Arabidopsis thaliana* by non-invasive image analysis. *Plant Physiol. Biochem.* 37, 671–678.

Liu, Y.G., Mitsukawa, N., Oosumi, T., and Whittier, R.F. (1995). Efficient isolation and mapping of *Arabidopsis thaliana* T-DNA insert junctions by thermal asymmetric interlaced PCR. *Plant J* 8, 457–463.

Marcaida, M.J., Schlarb-Ridley, B.G., Worrall, J.A., Wastl, J., Evans, T.J., Bendall, D.S., Luisi, B.F., and Howe, C.J. (2006). Structure of cytochrome c<sub>6A</sub>, a novel dithio-cytochrome of *Arabidopsis thaliana*, and its reactivity with plastocyanin: implications for function. *J. Mol. Biol.* 360, 968–977.

Märschner, H. (2002). *Mineral Nutrition in Higher Plants* (London: Academic Press).

Matsudaira, P. (1987). Sequence from picomole quantities of proteins electroblotted onto polyvinylidene difluoride membranes. *J. Biol. Chem.* 262, 10035–10038.

Merchant, S., and Bogorad, L. (1987). Metal ion regulated gene expression: use of a plastocyanin-less mutant of *Chlamydomonas reinhardtii* to study the Cu(II)-dependent expression of cytochrome c-552. *EMBO J* 6, 2531–2535.

Merchant, S.S., Allen, M.D., Kropat, J., Moseley, J.L., Long, J.C., Tottey, S., and Terauchi, A.M. (2006). Between a rock and a hard place: trace element nutrition in *Chlamydomonas*. *Biochim. Biophys. Acta* 1763, 578–594.

Olesen, K., Ejdeback, M., Crnogorac, M.M., Kostic, N.M., and Hansson, O. (1999). Electron transfer to photosystem I from spinach plastocyanin mutated in the small acidic patch: ionic strength dependence of kinetics and comparison of mechanistic models. *Biochemistry* 38, 16695–16705.

Pesaresi, P., Varotto, C., Meurer, J., Jahns, P., Salamini, F., and Leister, D. (2001). Knock-out of the plastid ribosomal protein L11 in *Arabidopsis*: effects on mRNA translation and photosynthesis. *Plant J* 27, 179–189.

Puig, S., Andres-Colas, N., Garcia-Molina, A., and Penarrubia, L. (2007). Copper and iron homeostasis in *Arabidopsis*: responses to metal deficiencies, interactions and biotechnological applications. *Plant Cell Environ.* 30, 271–290.

Ramshaw, J.A., Brown, R.H., Scawen, M.D., and Boulter, D. (1973). Higher plant plastocyanin. *Biochim. Biophys. Acta* 303, 269–273.

Redinbo, M.R., Yeates, T.O., and Merchant, S. (1994). Plastocyanin: structural and functional analysis. *J. Bioenerg. Biomembr.* 26, 49–66.

Rensing, S.A., et al. (2008). The *Physcomitrella* genome reveals evolutionary insights into the conquest of land by plants. *Science* 319, 64–69.

Schägger, H., and von Jagow, G. (1987). Tricine-sodium dodecyl sulfate-polyacrylamide gel electrophoresis for the separation of proteins in the range from 1 to 100 kDa. *Anal. Biochem.* 166, 368–379.

Schlarb-Ridley, B.G., Nimmo, R.H., Purton, S., Howe, C.J., and Bendall, D.S. (2006). Cytochrome  $c_{6A}$  is a funnel for thiol oxidation in the thylakoid lumen. *FEBS Lett.* 580, 2166–2169.

Schöttler, M.A., Kirchhoff, H., and Weis, E. (2004). The role of plastocyanin in the adjustment of the photosynthetic electron transport to the carbon metabolism in tobacco. *Plant Physiol.* 136, 4265–4274.

Seigneurin-Berney, D., et al. (2006). HMA1, a new Cu-ATPase of the chloroplast envelope, is essential for growth under adverse light conditions. *J. Biol. Chem.* 281, 2882–2892.

Shevchenko, A., Wilm, M., Vorm, O., Jensen, O.N., Podtelejnikov, A.V., Neubauer, G., Mortensen, P., and Mann, M. (1996). A strategy for identifying gel-separated proteins in sequence databases by MS alone. *Biochem. Soc. Trans.* 24, 893–896.

Sherman, F. (1991). Getting started with yeast. *Methods Enzymol.* 194, 3–21.

Shikanai, T., Muller-Moule, P., Munekage, Y., Niyogi, K.K., and Pilon, M. (2003). PAA1, a P-type ATPase of *Arabidopsis*, functions in copper transport in chloroplasts. *Plant Cell* 15, 1333–1346.

Shosheva, A., Donchev, A., Dimitrov, M., Zlatanov, I., Toromanov, G., Getov, V., and Alexov, E. (2004). Experimental and numerical study of the poplar plastocyanin isoforms using Tyr as a probe for electrostatic similarity and dissimilarity. *Biochim. Biophys. Acta* 1698, 67–75.

Shosheva, A., Donchev, A., Dimitrov, M., Kostov, G., Toromanov, G., Getov, V., and Alexov, E. (2005). Comparative study of the stability of poplar plastocyanin isoforms. *Biochim. Biophys. Acta* 1748, 116–127.

Taneva, S.G., Donchev, A.A., Dimitrov, M.I., and Muga, A. (2000). Redox- and pH-dependent association of plastocyanin with lipid bilayers: effect on protein conformation and thermal stability. *Biochim. Biophys. Acta* 1463, 429–438.

Thompson, J.D., Higgins, D.G., and Gibson, T.J. (1994). CLUSTAL W: improving the sensitivity of progressive multiple sequence alignment through sequence weighting, position-specific gap penalties and weight matrix choice. *Nucleic Acids Res.* 22, 4673–4680.

Wastl, J., Bendall, D.S., and Howe, C.J. (2002). Higher plants contain a modified cytochrome  $c_6$ . *Trends Plant Sci.* 7, 244–245.

Weigel, M., Varotto, C., Pesaresi, P., Finazzi, G., Rappaport, F., Salamini, F., and Leister, D. (2003). Plastocyanin is indispensable for photosynthetic electron flow in *Arabidopsis thaliana*. *J. Biol. Chem.* 278, 31286–31289.

Yu, J., et al. (2005). The Genomes of *Oryza sativa*: a history of duplications. *PLoS Biol.* 3, e38.

Zhang, L., Pakrasi, H.B., and Whitmarsh, J. (1994). Photoautotrophic growth of the cyanobacterium *Synechocystis* sp. PCC 6803 in the absence of cytochrome c553 and plastocyanin. *J. Biol. Chem.* 269, 5036–5042.

Zhou, J., and Goldsbrough, P.B. (1995). Structure, organization and expression of the metallothionein gene family in *Arabidopsis*. *Mol. Gen. Genet.* 248, 318–328.